



## Pharmaceutical Nanotechnology

## Synthesis and characterization of low-toxic amphiphilic chitosan derivatives and their application as micelle carrier for antitumor drug

Meirong Huo<sup>1</sup>, Yong Zhang<sup>1</sup>, Jianping Zhou\*, Aifeng Zou, Di Yu, Yiping Wu, Jing Li, Hong Li

Department of Pharmaceutics, China Pharmaceutical University, No. 24, Tongjiaxiang, 210009, Nanjing, China

## ARTICLE INFO

## Article history:

Received 9 February 2010

Received in revised form 22 April 2010

Accepted 4 May 2010

Available online 8 May 2010

## Keywords:

N-octyl-O-glycol chitosan

Self-assembly

Drug delivery

Safety

## ABSTRACT

A new series of amphiphilically modified chitosan molecules with long alkyl chains as hydrophobic moieties and glycol groups as hydrophilic moieties (N-octyl-O-glycol chitosan, OGC) was synthesized for use as drug carriers. The chemical structure was characterized by Fourier transform infrared, <sup>1</sup>H nuclear magnetic resonance, and elemental analysis. OGC could easily self-assemble to form nanomicelles in an aqueous environment and exhibited a low critical micellar concentration of 5.3–32.5 mg/L. The biocompatibility and low toxicity of OGC as excipient for the dosage forms aimed at i.v. administration were confirmed by hemolysis, acute toxicity and histopathological studies. Furthermore, the possibility of solubilizing paclitaxel (PTX), a water-insoluble antitumor drug, with OGC micelles was also explored. PTX was successfully loaded into OGC micelles by using a simple dialysis process. The drug-loading capacity of OGC and stability of drug-loaded micelles were significantly affected by the degree of substitution of alkyl chains. Moreover, a series of safety studies including hemolysis, hypersensitivity, maximum tolerated dose, acute toxicity, and organ toxicity revealed that the PTX-loaded OGC micelles had advantages over the commercially available injectable preparation of PTX (Taxol®), in terms of low toxicity levels and increased tolerated dose. Additionally, cytotoxicity studies showed that the PTX-loaded OGC micelles were comparable to the commercial formulation, but the blank micelles were far less toxic than the Cremophor EL vehicle. These results suggest that OGC is a promising carrier for injectable PTX micelles.

© 2010 Elsevier B.V. All rights reserved.

## 1. Introduction

To deliver poorly water-soluble drugs efficiently has been one of the most challenging goals for formulation scientists (Fahr and Liu, 2007; Fransson and Green, 2008). Paclitaxel (PTX) is an important clinical anticancer drug that exhibits strong cytotoxic activity against a variety of cancer types, especially breast and ovarian cancer (Wang et al., 2008). However, its clinical applications have been hindered by its extremely low solubility in water (0.3 µg/mL) (Feng and Huang, 2001). To enhance its solubility, PTX is currently formulated as a 50:50 mixture of Cremophor EL (a polyethoxylated castor oil) and ethanol (Taxol®). However, the amount of Cremophor EL required to solubilize PTX is considerably high (26 mL of Cremophor EL for an average patient for a single intravenous dose) (Gelderblom et al., 2001), which results in significant side effects such as hypersensitivity, neurotoxicity, nephrotoxicity, and cardiotoxicity. Therefore, a number of alternative formulations have been investigated aimed at solubilizing PTX: liposome (Marcel Musteata and Pawliszyn, 2006), lipid emulsion (Han et al., 2007),

mixed micelle (Wang et al., 2008), cyclodextrin complex (Bouquet et al., 2007), paclitaxel conjugate (Kakinoki et al., 2008), and polymeric micelles (Licciardi et al., 2006). These carriers did not only solubilize PTX but also may give targeted delivery after intravenous administration as a result of the enhanced permeability and retention (EPR) effect.

Recently, polymeric micelles have attracted increasing attention as promising vehicles for poorly soluble drugs (Kadam et al., 2009). Polymeric micelles are self-assemblies of amphiphilic block copolymers in aqueous media. The high potential of polymeric micelles as drug carriers lies in their unique characteristics such as nanoscale size, thermodynamic stability and unique core-shell architecture (Gao et al., 2008; Ye et al., 2009). Hydrophobic drugs can be solubilized into the hydrophobic core structures of polymer micelles. The hydrophilic shell surrounding the micellar core can prevent intermicellar aggregation or precipitation, protein adsorption, and cell adhesion from happening (Mahmud et al., 2007; Qiu et al., 2009). It has been reported that highly tumor-specific delivery of anticancer agents was achieved using polymeric micelles as carriers, following a passive targeting mechanism (Alexis et al., 2008; Kawano et al., 2006). Although much effort has been made to develop novel polymeric amphiphiles, only limited polymer amphiphiles are suitable as drug delivery vehicles because of the requirement for biocompatibility and biodegradability (Branco

\* Corresponding author. Tel.: +86 25 83271102; fax: +86 25 83301606.

E-mail address: [zhoujianp60@126.com](mailto:zhoujianp60@126.com) (J. Zhou).<sup>1</sup> These authors contributed equally to this work.

and Schneider, 2009). Additionally, low stability has been observed for drug-loaded polymer micelles in aqueous solution, and stability decreased as drug-loading levels increased (Huh et al., 2005).

Chitosan, one of the most plentiful biomaterials prepared from N-deacetylation of chitin, has attracted significant interest in biotechnology fields because of its well-known low toxicity, excellent biocompatibility and biodegradability (Kumar et al., 2000; Mi et al., 2002). To date, several hydrophobically modified chitosan derivatives, such as stearic acid-modified chitosan (Hu et al., 2006c), deoxycholic acid-modified chitosan (Lee et al., 2005), linolenic acid-modified chitosan (Chen et al., 2003; Liu et al., 2005), have been synthesized and confirmed to form micelle-like structures by self-aggregation in aqueous environment. These micelles showed good loading capacities for anionic macromolecules, e.g., gene (Cheong et al., 2009; Hu et al., 2006c) or protein (Hu et al., 2006a) and enhanced intracellular delivery abilities because of their cationic property and special spatial structure with multi-hydrophobic cores (Hu et al., 2008b, 2006c). However, only a small section of the hydrophobic segment can be conjugated to chitosan backbone (degree of substitution, DS <10%) because of the extremely low solubility of chitosan in neutral media (Liu et al., 2003), which led to low loading capacities of the micelles for nonionic hydrophobic drugs (Du et al., 2009; Hu et al., 2006b).

To overcome the above disadvantages, chitosan can be amphiphilically modified by attaching both hydrophobic and hydrophilic segments to the backbone. In our previous studies, we found that alkyl chain-modified succinyl chitosan (Xu et al., 2007) and carboxymethyl chitosan (Zhang et al., 2009) showed excellent drug-loading capacities because the alkyl chains had good affinities for hydrophobic drugs. I.C. Kwon's group synthesized cholan acid (Min et al., 2008; Nam et al., 2009), and deoxycholic acid-modified glycol chitosan (Kim et al., 2005a), and F.Q. Hu's group designed stearic acid-modified chitosan-g-polyethylene glycol (Hu et al., 2008a). Both groups found that positive charges were favorable to the interaction between micelles and cells (Hu et al., 2008a; Lee et al., 2009; Nam et al., 2009). Therefore, it seemed appropriate to explore the possibility of alkyl-modified hydrophilic chitosan with positive charges as a potential micellar drug delivery system.

In this study, we designed an amphiphilically modified chitosan derivative, N-octyl-O-glycol chitosan (OGC) and tested the potential of polymeric micelles composed of OGC as intravenously injectable carriers of PTX. Firstly, hydrophobic alkyl chains and hydrophilic glycol groups were conjugated to the chitosan backbone, respectively, and the self-assembling abilities and biocompatibilities of the chitosan amphiphilic derivatives were evaluated. Secondly, the effect of DS of alkyl chains of OGC on drug-loading capacity, stability, *in vitro* drug release, and other physicochemical properties were investigated in detail. Finally, the safety and *in vitro* cytotoxicity of blank OGC micelles and the PTX-loaded OGC micelles were evaluated using the Cremophor-EL-based commercial formulation (Taxol) as a control.

## 2. Materials and methods

### 2.1. Materials

Chitosan was purchased from the Zhejiang Yuhuan Biochemical Co. Ltd. (Zhejiang, China) with deacetylation degree of 90% and viscosity average molecular weight of  $8.7 \times 10^4$  Da. Octaldehyde was purchased from Nanjing Skyrun Golden Harvest Perfume Manu Co. Ltd. (Jiangsu, China). Sodium borohydride and ethylene oxide were purchased from Sinopharm Chemical Reagent Co., Ltd. (Shanghai, China). Pyrene was purchased from Fluka Company (>99%). PTX was obtained from Chongqing Meilian Pharm Co., Ltd. (Chongqing, China). Cremophor EL was a kind gift from

BASF Corp. (Ludwigshafen, Germany). Taxol (Bristol-Myers Squibb, New York, NY) was purchased in a retail pharmacy. Tween 80 was obtained from Jiangsu Chenpai Pharmaceutical Co. Ltd. (Jiangsu, China). 3-(4,5-Dimethylthiazol-2-yl)-2,5-diphenyltetrazolium bromide (MTT) was purchased from Sigma-Aldrich (St. Louis, MO). All other reagents were analytical grade and used without further purification. Distilled or deionized water was used in all experiments.

### 2.2. Animals

Kunming mice (18–22 g) were obtained from New Drug Screening Center of China Pharmaceutical University, and guinea pigs (250–300 g) were obtained from the Laboratory Animal Center of Nanjing General Hospital. All animals were pathogen free and allowed free to access food and water. The experiments were carried out in compliance with the National Institutes of Health Guide for the Care and Use of Laboratory Animals.

### 2.3. Synthesis of chitosan amphiphiles

#### 2.3.1. Synthesis of N-octyl chitosan

Chitosan was alkyl modified by the method described previously with slight modification (Liu et al., 2006). In brief, 2 g of chitosan were dissolved in 200 mL of 1% acetic acid solution. A predetermined amount of octaldehyde was added to the solution, and the mixture was stirred for 30 min. Hydrogenation was performed with sodium borohydride (0.64 g) dissolved in 6.4 mL of water. After a further 12 h of continuous stirring, the mixture was neutralized with 2 M sodium hydroxide. The precipitate was filtered and washed with methanol/water (80:20 and 90:10, v/v), methanol, hexane, and acetone, respectively. The product, N-octyl-chitosan (OC), was dried in vacuum.

#### 2.3.2. Synthesis of OGC

OGC was synthesized by conjugating glycol groups to OC. Briefly, 1 g of OC was suspended in 15 mL of 1% acetic acid solution, then 10 mL of 12.5 M sodium hydroxide was added, and the mixture was stirred at 40 °C for 12 h. The flask was then equipped with a reflux condenser, and the reaction mixture was cooled in an ice bath with the subsequent addition of 10 mL of ethylene oxide. After continuously stirring the mixture for 4 h, the ice bath was removed, and the mixture was stirred for an additional 5 h at 40 °C. The supernatant was discarded, and 40 mL of distilled water were added. The pH of the solution was adjusted to pH 7.0 with 5 M sodium hydroxide solution, and the solution was dialyzed against distilled water by using a dialysis membrane with a molecular weight cut-off of 14,000 Da. OGC was obtained by lyophilization.

### 2.4. Structure characterization of OGC

Fourier transform infrared (FT-IR) spectra were recorded with KBr pellets on a Nicolet Impact 410 spectrometer (Nicolet Analytical Instruments, Madison, WI).  $^1\text{H}$  nuclear magnetic resonance ( $^1\text{H}$  NMR) spectra were recorded with a Bruker Avance spectrometer (AV-500; Bruker, Karlsruhe, Germany) spectrometer operating at 500 MHz. Chitosan and OC were dissolved in the mixture of  $\text{D}_2\text{O}$  and DCl, respectively. OGC was dissolved in  $\text{D}_2\text{O}$ . Degree of substitution (DS), defined as the number of glycol groups or octyl chains per 100 glucosamine units of chitosan, was determined by elemental analysis by using a Vario EL III analyzer (Elementar, Hanau, Germany).

## 2.5. Determination of the critical micellar concentration

The critical micellar concentration (CMC) of OGC in distilled water was estimated by fluorescence spectroscopy by using pyrene as a hydrophobic fluorescence probe (Wilhelm et al., 1991). Briefly, 1 mL of pyrene solution ( $6 \times 10^{-6}$  M) in acetone was transferred into a 10-mL volumetric flask, and then acetone was removed from the solution by purging with nitrogen gas. Different amounts of OGC micelles were added into the volumetric flasks containing acetone-free pyrene, and the resulting solutions were diluted with distilled water to make the final pyrene and OGC concentrations of  $6 \times 10^{-7}$  M and  $1 \times 10^{-4}$  to 2 mg/mL, respectively. The solutions were sonicated for 30 min at 100 W followed by incubation at 40 °C for 1 h and kept from light overnight at room temperature for 12 h. Fluorescence spectra were recorded with an RF-5301 PC fluorescence spectrophotometer (Shimadzu, Kyoto, Japan) with the emission wavelength at 390 nm. The slit widths for emission and excitation were set at 3.0 and 1.5 nm, respectively. The peak height intensity ratio ( $I_3/I_1$ ) of the third peak ( $I_3$  at 338 nm) to the first peak ( $I_1$  at 333 nm) against the logarithm of micelles concentration was plotted.

## 2.6. Preparation of PTX-loaded OGC micelles

PTX-loaded OGC micelles were prepared by dialysis. Briefly, OGC powders (20 mg) were dispersed in 3 mL of distilled water under continuous stirring for 1.5 h at 50 °C until all powders were dissolved. PTX powders (30 mg) were dissolved in 1 mL of ethanol. The above polymer solution and a certain amount of PTX solution were mixed and sonicated with a probe-type ultrasonicator (JY92-2D; Ningbo Scientz Biotechnology Co., Ltd., Ningbo, China) at 100 W for 10 min in an ice bath. To remove ethanol, the resulting solution was dialyzed against distilled water overnight at room temperature by using a membrane with a molecular weight cut-off of 14,000. To remove unloaded PTX, the micellar solution was filtered through a 0.45- $\mu$ m filter and then lyophilized in the presence of 2% mannitol (Model LGJ-10, Gongyi Yuhua Instrument Co., Ltd., Gongyi, China). The lyophilized powders were kept in a refrigerator at 4 °C until use.

## 2.7. Characteristics of PTX-loaded OGC micelles

### 2.7.1. HPLC analysis

A Shimadzu LC-2010C system (Shimadzu, Kyoto, Japan) with built-in UV-vis detector was used to perform all the analyses. Chromatographic software Class VP 6.12 was used for data collection and processing. A Shimadzu VP-ODS (250 mm  $\times$  4.6 mm, 5  $\mu$ m) column was used for the separation. Mobile phase was composed of methanol and water (75:25); the flow rate and column temperature were set at 1 mL/min and 30 °C, respectively. The UV absorbance was determined at 227 nm.

### 2.7.2. Determining drug-loading capability

Drug-loading capability of the OGC micelles was determined using HPLC. Twenty microliters of PTX-loaded micelle solution was transferred into 10-mL volumetric flasks and diluted to mark with methanol. The solution was centrifuged at 10,000 rpm for 10 min, and the supernatant was analyzed with a validated HPLC assay. The drug-loading efficiency (DLE, %) and drug-loading content (DLC, wt.%) were calculated with the following equations:

$$\text{DLE (\%)} = \frac{\text{amount of PTX in micelles}}{\text{amount of PTX used for micelle preparation}} \times 100 \quad (1)$$

$$\text{DLC (wt.\%)} = \frac{\text{amount of PTX in micelles}}{\text{amount of PTX-loaded OGC micelles}} \times 100 \quad (2)$$

Because the solubility of free PTX is very low (<1  $\mu$ g/mL) compared to that of incorporated PTX as shown later (>2 mg/mL), the amount of free PTX in this preparation was not taken into account (Miwa et al., 1998; Zhang et al., 2004).

### 2.7.3. Particle size and zeta potential

The lyophilized powders were reconstituted with 5% dextrose injection solution. The particle size and zeta potential were measured using a Malvern Zetasizer 3000 system (Malvern Instruments Ltd., Malvern, UK). All of the dynamic light scattering (DLS) measurements were performed at 25 °C and at a scattering angle of 90°. The zeta potential values were calculated using the Smoluchowski equation.

### 2.7.4. Morphology

The morphology and particle size distribution were observed with transmission electron microscopy (TEM) using an H-7000 electron microscope (Hitachi, Tokyo, Japan) electron microscope operating at an accelerating voltage of 75 kV. Negative staining of samples was performed as follows: one drop of sample solution was placed onto a copper grid coated with carbon; the sample droplet was taped with a filter paper to remove surface water and air-dried for 5 min followed by an application of 0.01% phosphotungstic acid to get nanoparticles deposited on the grid. The samples were air-dried before observation.

### 2.7.5. Wide angle X-ray diffraction (WAXD) analysis

WAXD was performed using an XD-3A powder diffraction meter (Shimadzu, Kyoto, Japan) with Cu K $\alpha$  radiation. Samples were scanned from 2 to 40° 2 $\theta$  at a scanning speed of 1°/min and a step size of 0.05° 2 $\theta$ . The X-ray tube was operated at a potential of 40 kV and a current of 40 mA.

### 2.7.6. Stabilities of drug-loaded micelles after reconstitution

The *in vitro* stability of the micellar samples was determined by using a Cremophor-EL-based commercial formulation (Taxol) as a control. Lyophilized PTX-OGC micelle powders containing 0.8 mg PTX were dispersed in 1 mL of 5% dextrose. The resulting solution was incubated at 25 °C. Samples were taken from the solution at predetermined time points, and the particle size of PTX-loaded OGC micelles was measured by DLS. Then the samples were filtered through a 0.45- $\mu$ m filter to remove the large particles or precipitants. The resulting solution was diluted with methanol, and the concentration of PTX was determined by a validated HPLC assay, according to the method described above.

## 2.8. Safety of OGC amphiphiles and PTX-loaded OGC micelles

### 2.8.1. Hemolysis test

The hemolysis of OGC amphiphiles was determined by using low-molecular-weight surfactants (including Tween 80 and Cremophor EL) as controls. The hemolysis test was performed as described by Le Garrec D (Le Garrec et al., 2004). Human red blood cells (RBC) were collected from a healthy donor and kept in vacuum tubes (Shandong Weigao Orthopedic Device Co. Ltd., Weihai, China) containing 7.5% (w/v) K<sub>3</sub>EDTA. The human RBC suspension was centrifuged at 3000 rpm for 10 min. The cells were washed with saline and the suspension was centrifuged at 3000 rpm for 10 min, and the supernatant was discarded. The above process was repeated three times. The RBC suspension was diluted with saline to obtain a 2% suspension (v/v). RBC suspension (2.5 mL) was added to 2.5 mL of polymer samples until the ultimate concentrations of OGC, Tween 80, and Cremophore EL ranged from 0.2 to 4 mg/mL. After incubating at 37 °C for 3 h, the above suspension was centrifuged at 3000 rpm for 10 min to remove intact RBC. The supernatant was collected and analyzed for released hemoglobin with a UV-2450



spectrophotometer (Shimadzu) at 416 nm ( $n = 3$ ). To obtain 0 and 100% hemolysis, 2.5 mL of saline and 2.5 mL of distilled water was added to 2.5 mL of RBC suspension, respectively. The degree of hemolysis was calculated with the following equation (Cheon Lee et al., 2003):

$$\text{Hemolysis (\%)} = \frac{\text{Abs} - \text{Abs}_0}{\text{Abs}_{100} - \text{Abs}_0} \times 100 \quad (3)$$

where Abs, Abs<sub>100</sub>, and Abs<sub>0</sub> are the absorbance of samples, a solution of 100% hemolysis, and a solution of 0% hemolysis. The turbidity of samples was compensated for by using a sample solution without erythrocytes as a blank control.

Additionally, the hemolysis of PTX-loaded OGC micelles and Taxol were evaluated. RBC suspension (2.5 mL) was also added to 2.5 mL of above formulations, and the ultimate PTX concentrations ranged from 0.05 to 0.2 mg/mL.

### 2.8.2. Hypersensitivity test

Guinea pig model was used to evaluate the hypersensitivity of PTX-loaded OGC micelles by using Taxol as a control. Guinea pigs (250–300 g) were randomly assigned to the following three groups ( $n = 6$ , 50% male, 50% female): (1) negative control group, (2) PTX-OGC group, and (3) Taxol group. The animals were intramuscularly injected with a 5% dextrose solution for the negative control group, PTX-loaded OGC micellar solution (5.0 mg/mL in 5% dextrose, dosage 10 mg/kg) for the PTX-OGC group, and Taxol solution (5.0 mg/mL in 5% dextrose, dosage 10 mg/kg) for the Taxol group every other day. After the third injection, each group was further divided into two subgroups ( $n = 3$ ). The animals in subgroup 1 were intraperitoneally injected with 2–3-mL samples 14 days after the first injection, and the animals in subgroup 2 were intraperitoneally injected with 2–3-mL samples 21 days after the first injection. The anaphylactic response was observed after each injection.

### 2.8.3. Maximum tolerated dose (MTD) studies

The MTD for PTX-loaded OGC micelles and Taxol administered intravenously was investigated in healthy Kunming mice (18–22 g). The mice were randomly assigned to nine groups ( $n = 10$ , 50% male, 50% female) and received a single dose of Taxol at 20, 25, 30, and 40 mg/kg; PTX-OGC at 80, 90, 100, and 110 mg/kg; and dextrose 5% as a control through the tail vein. Drug effects were determined by closely monitoring weight changes and survival rates. The highest nonlethal dose of PTX causing <10% weight loss within 1 week of ceasing dosing was defined as the MTD. The animals showing weight loss exceeding 20% were sacrificed, as changes of this magnitude often indicate lethal toxicity (Freireich et al., 1966).

### 2.8.4. Acute toxicity

To evaluate the acute toxicity of OGC amphiphiles and PTX-loaded OGC micelles, their median lethal dose (LD<sub>50</sub>) of both blank OGC micelles and PTX-loaded OGC micelles was determined by using Taxol as a control. Kunming mice (18–22 g) were randomly divided into 14 groups ( $n = 10$ , 50% male, 50% female) and received a single injection of OGC micellar solution at the dose of 391.5, 460.6, 541.9, 637.5, and 750.0 mg/kg; PTX-loaded OGC micellar solution at the dose of 88.7, 104.4, 122.8, 144.5, and 170.0 mg/kg; Taxol at the dose of 39.4, 43.7, 48.6, 54.0, and 60.0 mg/kg; and dextrose 5% as a control through the tail vein. Mice were observed for 2 weeks in all groups, and the number of mice surviving was recorded. The LD<sub>50</sub> value and 95% confidence limits were calculated using Bliss method (Bliss, 1935).

The histopathological affects of blank OGC and PTX-loaded OGC micelles on various organs such as heart, liver, spleen, lung, and kidney were investigated after intravenous administration of OGC or PTX-loaded OGC micellar solution at a half-dose level of LD<sub>50</sub>. The histopathological changes in each organ were observed under

an Olympus BX-40 light microscope (Tokyo, Japan) at day 8 after the treatment.

## 2.9. Cytotoxicity

HepG2 cells were obtained from the American Type Culture Collection and were maintained in RPMI-1640 media at 37 °C in a 5% CO<sub>2</sub> humidified environment. For the 3-(4,5-dimethylthiazol-2-yl)-2,5-diphenyltetrazolium bromide (MTT) assay, cells were plated to confluence on 96-well plates and were allowed to adhere overnight.

*In vitro* cytotoxicity of PTX-loaded OGC and blank OGC micelles were evaluated by MTT assay in human hepatoma HepG2 cell lines by using Taxol, Taxol blank vehicle or free PTX solution as control (Diaz et al., 2006). Taxol blank vehicle was prepared as described previously (Carstens et al., 2008). Briefly, 1.0 mL of ethanol and 1.0 mL of Cremophor EL were mixed and then the mixture was sonicated for 30 min. PTX-loaded OGC micelles and Taxol were diluted with culture medium to obtain the desired PTX solution, whose concentration of PTX ranged from 0.0001 to 100 µg/mL. Blank OGC micelles and Taxol blank vehicle were diluted the same fold as their corresponding formulations containing drugs, respectively. Free PTX solution was prepared by dissolving a certain amount of PTX in methanol and diluted with culture medium to give a concentration of 0.0001–1 µg/mL (Cavallaro et al., 2003).

The cultured cells were incubated for 72 h in the presence of various amounts of the above samples. Then, 10 µL of MTT (5 mg/mL in PBS) was added, followed by incubating for 4 h. DMSO (100 µL) was added to each well to dissolve any formazan crystals formed. The plates were vigorously shaken before the relative color intensity was measured at the analysis wavelength of 570 nm and the reference wavelength of 630 nm using a microplate reader (Multiskan Mk3, Thermo Labsystems, Beverly, MA, USA). The toxicity of PTX formulations was expressed as the inhibitory concentration at which 50% of cell growth inhibition was obtained (IC<sub>50</sub>). The IC<sub>50</sub> was calculated using XLFit program using the one-site dose–response model 205. Each sample was tested in triplicate, six wells with only culture medium served as a blank, and the relative cell viability was calculated and presented as a percentage of control values.

## 2.10. Statistical analysis

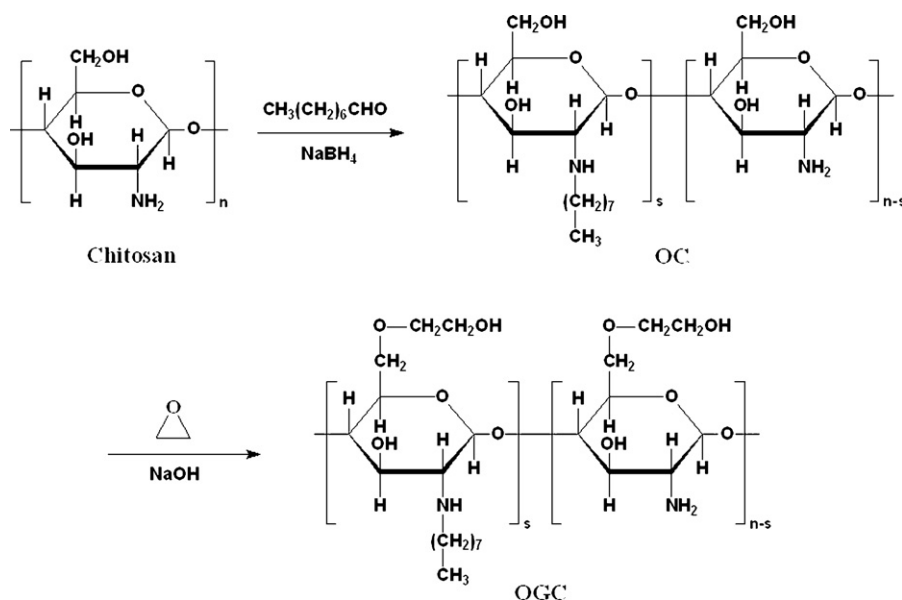
Statistical analysis was performed with Student's *t*-test for two groups and one-way ANOVA for multiple groups. All results were expressed as mean ± SD unless otherwise noted;  $P < 0.05$  was considered statistically significant.

## 3. Results and discussion

### 3.1. Synthesis and characterization of OGC

A new series of amphiphilically modified chitosan molecules with long alkyl chains as hydrophobic moieties and glycol groups as hydrophilic moieties were synthesized for use as drug carriers. Detailed schemes for the preparation of OGC are shown in Scheme 1. Chitosan was alkylated via Schiff bases formed by the reaction between the primary amino groups of chitosan and octaldehyde followed by reduction of the Schiff base intermediates with sodium cyanoborohydride. OGC was synthesized by reacting OC with ethylene oxide under alkaline conditions. By changing the feed ratio of octaldehyde to chitosan, OGCs with different DS values of alkyl chains were prepared.

The structure of synthesized polymer was determined by FT-IR and <sup>1</sup>H NMR. The FT-IR spectrum of chitosan (Fig. 1a) showed a broad –OH stretch absorption band between 3500 and 3100 cm<sup>–1</sup> and the aliphatic C–H stretch between 2990 and 2850 cm<sup>–1</sup>. As the



Scheme 1. Scheme of synthesis of OGC.

O–H stretch band and N–H stretch band were aligned, it appeared as a broad band from 3450 and 3100  $\text{cm}^{-1}$  in the spectrum. Other major absorption bands between 1229 and 1041  $\text{cm}^{-1}$  represented the free primary amino group ( $-\text{NH}_2$ ) at the C2 position. The peak at 1655  $\text{cm}^{-1}$  represented the acetylated amino group of chitin, which indicated that the sample was not fully deacetylated. The peak at 1384  $\text{cm}^{-1}$  represented the  $-\text{C}-\text{O}$  stretch of primary alcoholic group ( $-\text{CH}_2-\text{OH}$ ). In the IR spectrum of OC (Fig. 1b), the characteristic band of  $-\text{NH}_2$  at 3300, 1601, and 1078  $\text{cm}^{-1}$  disappeared or significantly decreased after chitosan was alkylated, indicating the

substitution reaction occurred on  $\text{NH}_2$  moieties. Meanwhile, the stronger peaks at 2925 and 2854  $\text{cm}^{-1}$  of the OC spectrum could be assigned to the aliphatic C–H stretch band, which indicated that alkyl chains were successfully conjugated to the primary amino of chitosan. In the IR spectrum of OGC (Fig. 1c), the absorption at 2927, 2856, 1450, and 1383  $\text{cm}^{-1}$  became much stronger, which indicated that a large number of methylene was introduced to the OC. The new strong absorption between 1210 and 1000  $\text{cm}^{-1}$  was attributed to the C–O stretch band and C–O–C asymmetric stretching vibration. The result indicated that the etherification occurred mainly at the C6–OH of chitosan (Huang et al., 2005).

The successful incorporation of the octyl and glycol groups onto the chitosan backbone was further ascertained by  $^1\text{H}$  NMR assay of chitosan, OC, and OGC. As shown in Fig. 2, the peaks in the  $^1\text{H}$  NMR spectrum of the D-glucosamine unit of chitosan were nearly identical to those in previous reports (Chen et al., 2004), and the peaks could be assigned as follows: 2.0 ( $-\text{CH}_3$ , acetyl group), 4.7 (1-H), 3.1 (2-H), and 3.5–3.9 (3-H–6-H). Based on the chitosan spectrum, the signals at 3.0–3.4 and 1.1–2.0 ppm in the OC spectrum were assigned to the methylene hydrogen ( $-\text{NH}-\text{CH}_2-(\text{CH}_2)_6-\text{CH}_3$ ) and ( $-\text{NH}-\text{CH}_2-(\text{CH}_2)_6-\text{CH}_3$ ) of the N-alkyl group, respectively. The peak at 0.95 ppm was attributed to the methyl hydrogen ( $-\text{NH}-\text{CH}_2-(\text{CH}_2)_6-\text{CH}_3$ ). Based on the spectra of OC, the resonances in the range of 3.5–4.2 ppm of the OGC spectrum were attributed to the protons of the glycol group ( $-\text{O}-\text{CH}_2-\text{CH}_2-\text{OH}$ ), ( $-\text{O}-\text{CH}_2-\text{CH}_2-\text{OH}$ ), and chitosan backbone (2-H–5-H). The data from  $^1\text{H}$  NMR demonstrated that the substitution of alkyl chains and glycol group occurred mainly at the amino group and hydroxyl group of chitosan, respectively.

The DS of the octyl and glycol groups was calculated based on the elemental analysis data by comparing the C and N molar ratio obtained from elemental analysis using the following equations (Senso et al., 2000):

$$\text{DS of alkyl group (\%)} = \frac{\text{C/N(mol)}_{\text{OC}} - \text{C/N(mol)}_{\text{Chitosan}}}{8} \times 100(4)$$

$$\text{DS of glycol group (\%)} = \frac{\text{C/N (mol)}_{\text{OGC}} - \text{C/N (mol)}_{\text{OC}}}{2} \times 100(5)$$

All results are shown in Table 1. OGC-1, OGC-2 and OGC-3 indicates OGC with DS of the octyl groups 24.2%, 41.5% and 58.7%, respectively. The DS of the glycol group was near 100% for all the three samples.

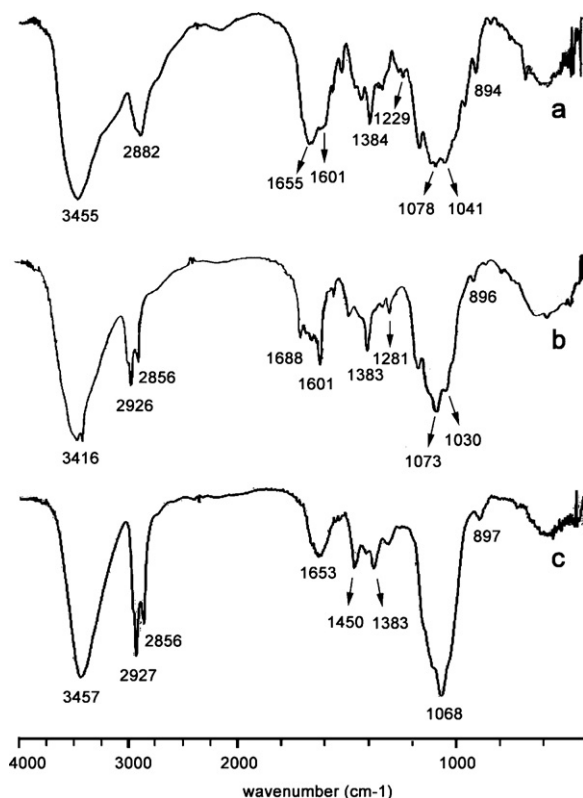
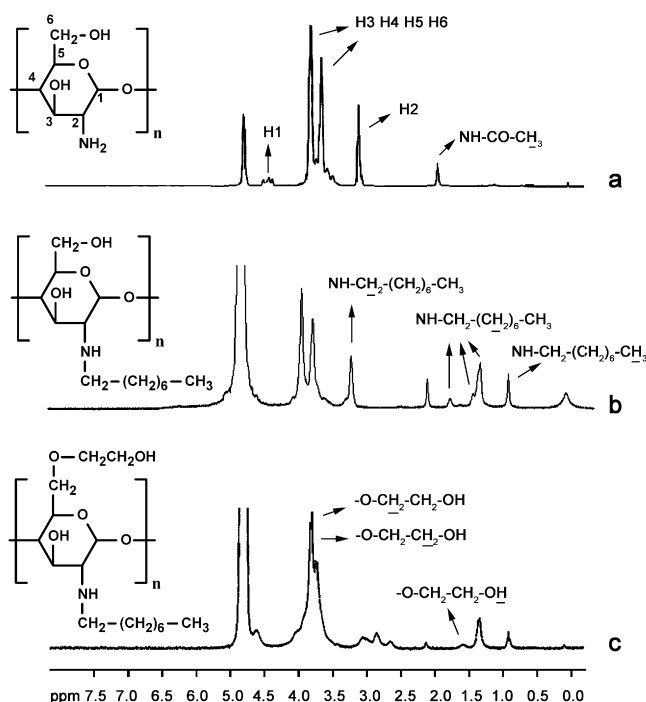


Fig. 1. FT-IR spectra of (a) chitosan, (b) OC and (c) OGC.

**Table 1**  
Chemical compositions and properties of OGC micelles.

Sample	DS of glycol groups (%)	DS of octyl chains (%)	Size (nm)	Polydispersity index	Zeta potential (mV)	CMC (mg/L)
OGC-1	105.7	24.2	228.3	0.148	+30.2	32.5
OGC-2	102.4	41.5	204.2	0.119	+28.6	19.8
OGC-3	103.8	58.7	190.7	0.132	+24.6	5.3



**Fig. 2.**  $^1\text{H}$  NMR spectra of (a) chitosan in  $\text{D}_2\text{O}/\text{DCl}$ , (b) OC in  $\text{D}_2\text{O}/\text{DCl}$  and (c) OGC in  $\text{D}_2\text{O}$ .

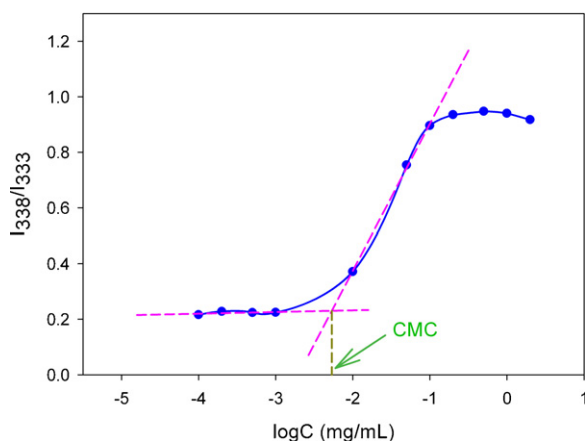


**Fig. 3.** Plot of the quotient of vibrational band intensities ( $I_{338}/I_{333}$ ) from excitation of pyrene as a function of  $\log C$  of OGC-3 in distilled water.

### 3.2. Self-assembly of OGC amphiphiles

Micelles can be formed only when the concentration of polymer is higher than its CMC, which plays an important role in maintaining the stability of micellar system. Polymeric micelles are generally more stable than low-molecular-weight surfactant micelles because of their markedly lower CMC. To determine the CMC of OGC, fluorescence was measured using pyrene as a probe. Fig. 3 shows a typical plot of  $I_{338}/I_{333}$  vs.  $\log(C)$  of OGC. A substantial increase of the intensity ratio was observed when the concentra-

tion was higher than the CMC value, which indicated nanomicelle formation. Therefore, CMC was estimated as the interception of two straight lines, one of which was the fitted line at low nanoaggregate concentrations and the other was the fitted line on the rapid rising part of the curve.

As shown in Table 1, CMC of OGC was in the range 5.3–32.5 mg/L, depending on the quantity of hydrophobic groups. As the DS of the hydrophobic alkyl chains increased, the CMC of OGC significantly decreased. A greater degree of hydrophobic substitution in the macromolecules of OGC might facilitate self-aggregation, which favors hydrophobic interactions and, thus, the formation of dense polymeric micelles.

The CMC of OGC was also significantly lower than that of low-molecular-weight surfactants (e.g.,  $1.0 \times 10^3$  mg/L for deoxycholic acid vs.  $2.3 \times 10^3$  mg/L for sodium dodecyl sulfate in water (Lee et al., 1998)) and comparable to or even lower than that of chitosan amphiphiles, such as deoxycholic acid-modified glycol chitosan with a CMC of 47–219 mg/L (Kim et al., 2005b) and deoxycholic acid-modified chitosan with a CMC of 13.2–44.7 mg/L (Lee et al., 1998). The low CMC of OGC was attributed to the higher DS of alkyl chains with stronger hydrophobicity. The results suggested that the OGC micelles may remain stable in solution, even after extreme dilution, and preserve their stability without dissociation after i.v. injection into systemic circulation.

### 3.3. Preparation of PTX-loaded OGC micelles

PTX was incorporated into OGC micelles by using a simple dialysis method. DLE and DLC were measured by a validated HPLC assay. The detailed effects of drug-to-polymer ratio on DLE and DLC are shown in Table 2. When the initial weight ratio of PTX to polymer increased from 0.4:2 to 1:2, the amount of PTX introduced into OGC micelles significantly increased from 15.7 wt.% to 32.8 wt.%. When the initial weight ratio of PTX to polymer exceeded 1:2, for example, up to 1.5:2, there was significant aggregation of unloaded PTX during the preparation of drug-loaded micelles, which resulted in a decrease in the loading level of OGC. Therefore, the optimal feeding ratio of PTX to polymer was finalized as 1:2.

The effect of the amount of the hydrophobic group of OGC amphiphiles on DLE and DLC was further investigated. As shown in Table 2, micelles prepared with the OGC having an octyl DS range of 24.2–58.7% had DLE values of 62.7–91.9% and DLC values of 23.9–32.8 wt.%. Higher DS of alkyl chains favored the formation of inner cores with larger hydrophobic space, which may provide the micelles an enhanced capacity to accommodate hydrophobic drugs.

The solubility of PTX in water was increased successfully to multiple times its inherent solubility after being loaded into micelles. For instance, 15 mg of the freeze-dried drug-loaded micelles (no mannitol) easily dissolved in 1 mL of distilled water in this study (higher concentrations might be possible). At the loading level of 32.8 wt.%, the effective concentration of PTX could be 4.9 mg/mL, which is  $1.6 \times 10^4$  times higher than its intrinsic water solubility of 0.3  $\mu\text{g}/\text{mL}$  (Seow et al., 2007). This observation confirmed the presence of hydrophobic cores, otherwise, such a high concentration of PTX in water would not have been achieved (Branco and Schneider, 2009; Mahmud et al., 2007). The highest DLC value (32.8 wt.%) observed in the OGC micellar system was considerably higher than those of most of micelles reported for solubilizing

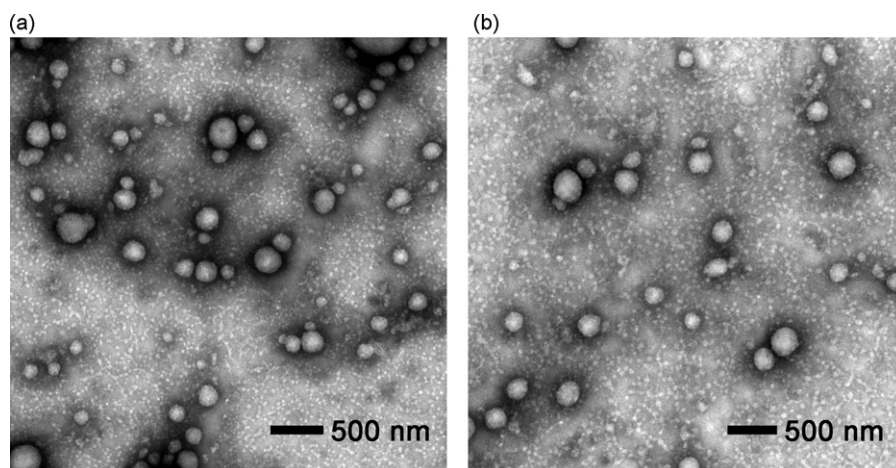


Fig. 4. TEM images of (a) OGC-3 micelles and (b) PTX-OGC-3 micelles.

PTX (DLC 5–25 wt.%) (Danhier et al., 2009; Kim et al., 2006; Li et al., 2007; Saravanakumar et al., 2009; Zhang et al., 2004; Zhao et al., 2009). The compatibility between the guest molecule and the core-forming block is thought to be the most important factor influencing the DLC of polymeric micelles (Le Garrec et al., 2004). This good loading capacity of OGC micelles might be attributed to the high DS values of alkyl chains and good affinity between alkyl chains and PTX. In addition, it is worth noting that, besides excellent drug-loading capacity, the DLE of OGC was quite high (>90%). Considering the resource scarcity and expense of PTX, a high drug DLE value will be beneficial in reducing the final product cost.

### 3.4. Characterization of PTX-loaded OGC micelles

#### 3.4.1. DLS and morphology

The particle size and polydispersity index of PTX-loaded OGC micelles were estimated by DLS. The sizes of PTX-loaded OGC micelles prepared with OGC of different DS of alkyl chains were significantly bigger than those of blank OGC micelles (Tables 1 and 2,  $P < 0.05$ ), which indicated that the drug was located inside the micelles. The particle size decreased as the DS of the alkyl chains increased, which indicated the formation of more intact hydrophobic cores, as a result of the enhanced interaction between hydrophobic alkyl chains. It is also worth noting that the size of the drug-loaded micelles was not significantly affected by PTX concentration in the range of 0.1–2 mg/mL. This implied that the interparticle interaction between micelles was almost negligible. The polydispersity index of PTX-loaded OGC micelles, estimated by the cumulant method, was fairly low ( $< 0.182$ ), which suggested a narrow size distribution.

Zeta potential or particle surface charge is an important parameter indicating to the stability of nanocarrier systems. A relatively high surface charge may provide a repelling force between the particles, thus increasing the stability of the solution (Kim et al., 2003). As shown in Table 2, all the PTX-loaded OGC micelles had rela-

tively high positive zeta potentials of around +25 mV. It is obvious that the high positive zeta potential of micelles was attributed to the presence of ionized amino groups distributing on the surface of micelles, which indicated that positive-charged glycol chitosan covered the micelles. It is reasonable to conclude that the charged particles may repel each other and prevent aggregation or precipitation happening, thus resulting in good stability.

TEM was used to visualize directly the size and morphology of OGC micelles with or without drug (Fig. 4). Smooth sphere morphology was observed for OGC and PTX-loaded OGC micelles. It was also noted that the size of blank OGC micelles or PTX-loaded OGC micelles determined with TEM may be smaller than that of intact micelles in an aqueous phase, because of the collapse of the outer shell during the drying process in TEM assay.

#### 3.4.2. WAXD analysis

To confirm the existence of PTX in the polymeric micelles, WAXD analysis were conducted for PTX, blank micelles, PTX-loaded micelles, and the physical mixture of blank micelles and PTX, respectively. As shown in Fig. 5, OGC gave two intense peaks at  $2\theta$  of  $12.95^\circ$  and  $13.90^\circ$  (Fig. 5a). PTX showed seven intense peaks at  $2\theta$  of  $5.45^\circ$ ,  $9.05^\circ$ ,  $9.80^\circ$ ,  $10.20^\circ$ ,  $11.20^\circ$ ,  $12.55^\circ$ , and  $13.80^\circ$  and numerous small peaks between  $15^\circ$  and  $25^\circ$  (Fig. 5b). When the two samples were physically mixed at the ratio of 68:32 (w/w), typical crystal peaks of PTX and modified chitosan were still observed (Fig. 5c). The lyophilized drug-loaded micellar system had no PTX peaks, but it had two peaks similar to those of the lyophilized blank micellar system (Fig. 5d). Therefore, it can be concluded that PTX molecules were mixed uniformly with polymer molecules or PTX existed inside micelles in an amorphous state.

#### 3.4.3. Stability of PTX-loaded OGC micelles after reconstitution

Most polymer micelles have poor physical stability after drug loading. In general, the stability of polymer micellar systems decreases as DLC increases. OGC micelles possessed an extremely

Table 2  
PTX loading into OGC micelles. Data are presented as mean  $\pm$  SD ( $n = 3$ ).

Polymer	Feed weight ratio of PTX:OGC (w/w)	DLE (%)	DLC (wt.%)	Size (nm)	Polydispersity index	Zeta potential (mV)
OGC-3	0.4:2	$92.8 \pm 1.3$	$15.7 \pm 0.2$	$194.5 \pm 4.4$	$0.139 \pm 0.005$	$+26.1 \pm 1.8$
OGC-3	0.7:2	$91.3 \pm 1.4$	$24.2 \pm 0.3$	$200.8 \pm 3.9$	$0.153 \pm 0.004$	$+25.8 \pm 1.4$
OGC-3	1:2	$91.9 \pm 2.5$	$32.8 \pm 0.6$	$210.4 \pm 5.1$	$0.147 \pm 0.005$	$+26.4 \pm 1.4$
OGC-3	1.5:2	$55.2 \pm 4.3$	$29.3 \pm 1.6$	$205.5 \pm 7.4$	$0.182 \pm 0.006$	$+26.2 \pm 1.6$
OGC-1	1:2	$62.7 \pm 1.8$	$23.9 \pm 0.5$	$245.3 \pm 4.3$	$0.156 \pm 0.005$	$+28.8 \pm 1.6$
OGC-2	1:2	$79.5 \pm 1.7$	$28.4 \pm 0.4$	$215.7 \pm 4.9$	$0.163 \pm 0.006$	$+27.9 \pm 1.3$



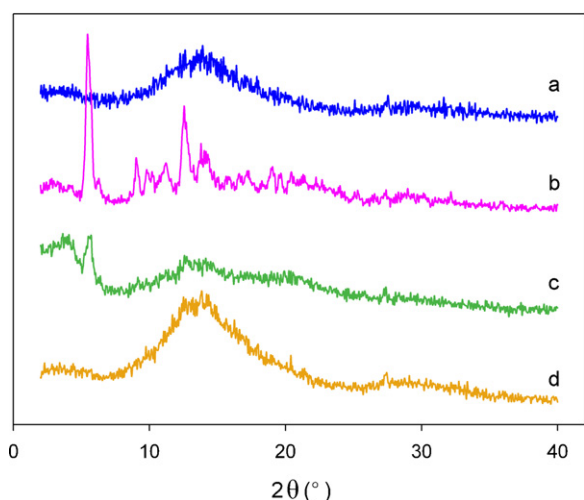


**Fig. 5.** Powder X-ray diffraction patterns for the lyophilized powder: (a) the lyophilized blank OGC-3 micelles; (b) PTX; (c) physical mixture of blank micelles and PTX (68:32, w/w); (d) PTX-loaded OGC-3 micelles (32.8 wt.% drug loading).

high drug-loading capacity, and therefore it was necessary to further investigate their *in vitro* stability. The loading content of PTX in micelles was observed as a function of time after reconstitution to test the stability of the drug-loaded micelles by using the Cremophor EL-based commercial formulation Taxol as a control. As shown in Fig. 6a, Taxol showed poor physical stability, as some particles slowly precipitated out of the aqueous solution after being stored at 25 °C for 24 h, and the amount of PTX dissolved in the solution was almost reduced to 0 after 2 days. Similar results, that Taxol® maintained its stability only for about 1 day have been reported earlier (Pourroy et al., 2005). Hence, an in-line filter was recommended for intravenous administration, and Taxol should be administered promptly after dilution (Stanford and Hardwicke, 2003). Even though the DLC was >30 wt.%, the drug-loaded OGC micellar system could still maintain its stability without drug precipitation for up to 5 days at 25 °C. Such high loading capacity plus high stability in aqueous media have seldom been reported. Polymeric micelles composed of poly(lactic acid)-*b*-poly(ethylene glycol) (PLA-*b*-PEG), poly(D,L-lactic acid)-block-methoxypolyethylene glycol (PDLLA-*b*-mPEG), and poly(D,L-lactide)-block-poly(N-vinylpyrrolidone) (PDLLA-*b*-PVP), which have been shown to solubilize PTX, showed drug precipitation in less than 24 h with a DLC of 5–27 wt.% (Burt et al., 1999; Cavallaro et al., 2003; Huh et al., 2005; Liggins and Burt, 2002). The unique properties of OGC may be ascribed to two factors:

(1) the positively charged glycol chitosan with strong hydrophilicity constituted the surface of the micelles, which may have repelled each other and prevented aggregation or precipitation happening; and (2) the strong interaction between the hydrophobic alkyl chains and drugs reduced the leakage of drug from the inner core of micelles.

The excellent stability of drug-loaded OGC micelles was also confirmed by DLS measurement (Fig. 6b). In the first 5 days, there were no significant changes in particle size of drug-loaded micelles, while the polydispersity index increased slightly. On the sixth day, the particle size and polydispersity index increased significantly, especially for PTX-loaded OGC with the minimum number of alkyl chains. The result indicated that the increase in DS of alkyl chains enhances the hydrophobicity of inner cores, which may counteract micelle expansion.

### 3.5. Safety evaluation of blank OGC micelles and drug-loaded micelles

#### 3.5.1. Hemolysis

Because amphiphilic polymers are analogs of low-molecular-weight surfactants, they may have similar properties as surfactants, such as causing cell membrane damage following i.v. administration (Le Garrec et al., 2004). To determine whether OGC induces membrane damage, the level of hemolysis of OGC was compared with that of Tween 80 and Cremophore EL, which are typical surfactants used for i.v. administration (Le Garrec et al., 2004). Fig. 7a shows hemolysis at various concentrations of OGC-3, Tween 80, and Cremophore EL. As the concentration increased, hemolysis induced by Tween 80 increased dramatically. At the concentration of 4 mg/mL, hemolysis caused by Tween 80 reached 67.7%. OGC-3 and Cremophore EL were nonhemolytic *in vitro* toward human RBCs (6.3% and 0.4% hemolysis at 4 mg/mL, respectively). Because the maximum tolerated dose of Cremophore EL for i.v. administration is 75 mg/day, compared with 500 mg/day for Tween 80 (Miwa et al., 1998), Cremophore EL is considered more toxic than Tween 80, which might account for the serious side effects of Cremophore EL, such as hypersensitivity and neurotoxicity. OGC with different DS of alkyl chains showed similar hemolysis (data not shown), which suggested that these nanomicelles are not toxic toward erythrocytes after i.v. injection.

In addition, the hemolysis of PTX-loaded OGC-3 micelles was compared to the Cremophor-based commercial formulation. As shown in Fig. 7b, as the concentration of PTX increased in the range of 0.04–0.4 mg/mL, hemolysis induced by the commercial formulation increased from 3.2% to 25.3%, while hemolytic activity of PTX-loaded OGC-3 micelles was almost negligible (2.3% hemoly-

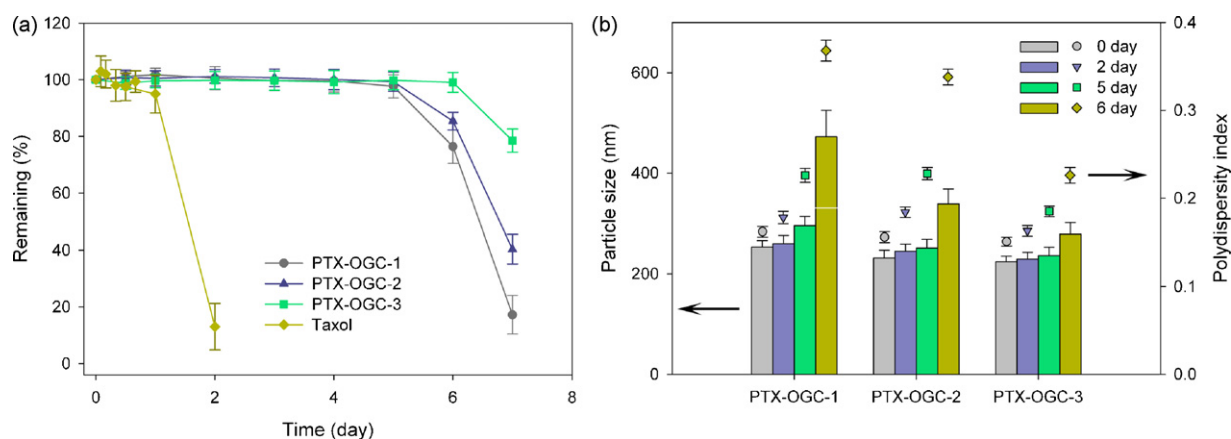


**Fig. 6.** (a) Loading content of PTX in micelles and (b) particle size as a function of time of PTX-loaded OGC micelles and Taxol in 5% dextrose at 25 °C ( $n=3$ ).



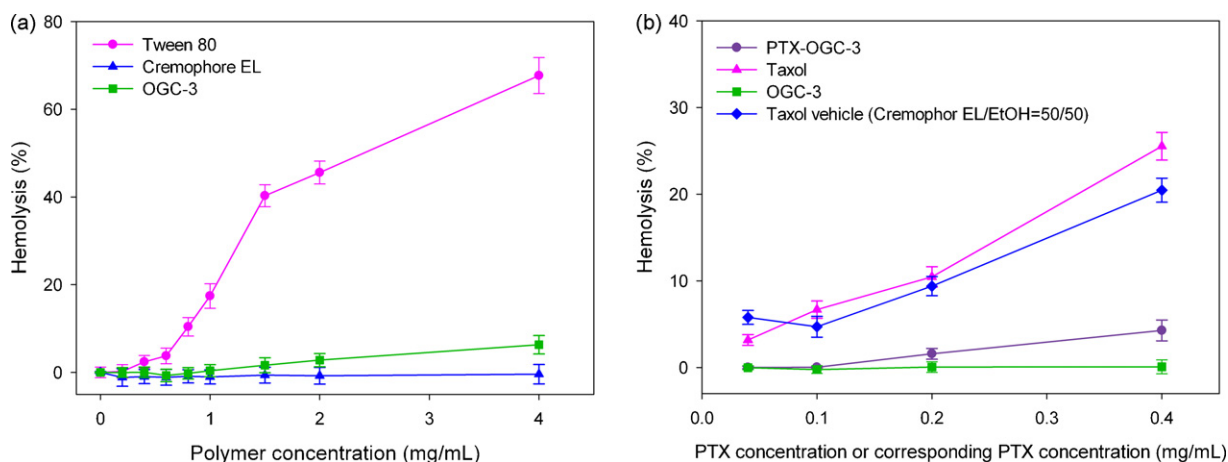


**Fig. 7.** Hemolysis as a function of concentration of (a) Tween 80, Cremophor EL and OGC-3; (b) PTX-loaded OGC-3 micelles, Taxol and their corresponding blank formulations ( $n = 3$ ).

sis). The results suggested that PTX-loaded OGC micelles were not toxic toward erythrocytes after i.v. injection. Although Cremophor EL showed no hemolysis even at the concentration of 4 mg/mL as described above, Cremophor EL/ethanol (50/50) showed similar hemolytic activity compared to the commercial formulation Taxol (Fig. 7b). Thus, the hemolysis of the commercial formulation could be attributed to the use of ethanol in the formulation.

### 3.5.2. Hypersensitivity test

PTX-OGC-3 (drug loading of 32.8 wt.%) was selected to evaluate hypersensitivity. A positive reaction was demonstrated by the occurrence of convulsion, collapse, circulatory collapse, and death or occurrence of at least two kinds of anaphylactic response such as piloerection, anhelation, sneezing, retching, and cough. The results demonstrated that the PTX-OGC-3-treated group and negative control group did not respond to the final challenge. However, in the Taxol group, typical anaphylaxis, such as anhelation and convulsion, occurred immediately after the first intramuscular injection, and five guinea pigs treated with Taxol died within 24 h. Therefore, pretreatment with corticosteroids and antihistamines was required before taking Taxol to reduce the risk of hypersensitivity reactions (Stanford and Hardwicke, 2003). These results demonstrated that the PTX-OGC-3 solution used at the concentration of 5.0 mg/mL did not cause hypersensitivity. In terms of hypersensitivity, PTX-loaded OGC micelles were superior to Taxol.

### 3.5.3. MTD

To determine the MTD of PTX formulations, higher doses of PTX-OGC-3 and Taxol were injected intravenously in healthy Kunming mice (Table 3). The MTD of PTX-OGC-3 or Taxol after a single injection was determined to be 100 mg/kg or 25 mg/kg, respectively. Death resulting from toxicity was observed at the dose of 110 mg/kg for PTX-OGC-3 and 40 mg/kg for Taxol. Furthermore, it was noted that all mice receiving Taxol at all dose levels showed severe prostration, apathy, respiratory distress, and catatonia after injection, whereas no apathy was observed in PTX-OGC-3 group at any dose level. In addition, severe prostration, apathy, respiratory distress, and catatonia were also found after treatment with the Cremophor vehicle (data not shown). Thus, toxicity appeared to be related to the use of Cremophor EL and dehydrated ethanol.

### 3.5.4. Acute toxicity

LD<sub>50</sub> has been used as a measurement to evaluate the acute toxicity. Mice were injected with various doses of OGC-3, PTX-OGC-3, or Taxol via tail vein. Toxic responses such as severe prostration, apathy, respiratory distress, catatonia and the number of mice

surviving were observed. The LD<sub>50</sub> of OGC-3 administered by intravenous injection was 551.1 mg/kg with the 95% confidence limits of 509.8–596.0 mg/kg. The LD<sub>50</sub> was very high because of its excellent capacity of solubilizing hydrophobic drugs such as PTX. For example, the drug-loading content of PTX in OGC-3 was 32.8 wt.%. In *in vivo* studies in mice, the dosage of PTX was no more than 20 mg/kg; therefore, the dosage of OGC-3 was no more than 40 mg/kg, which was much less than the LD<sub>50</sub> of OGC.

The LD<sub>50</sub> of PTX-OGC-3 administered by intravenous injection in mice was 123.1 mg/kg with the 95% confidence limits of 113.9–133.2 mg/kg. The LD<sub>50</sub> of Taxol was 50.7 mg/kg, which was 2.5-fold lower than that of PTX-OGC-3. The corresponding 95% confidence limits were 48.2–53.2 mg/kg. These parameters indicated that the PTX-loaded OGC micelles were less toxic than Taxol and provided critical guidelines for administering PTX-loaded OGC micelles in future studies. This finding was in good agreement with the above-mentioned MTD studies on mice, which demonstrated that PTX-loaded OGC micellar preparations were better tolerated.

To investigate the histopathological effect of OGC-3 and PTX-OGC-3 on various organs, such as heart, liver, spleen, lung, and kidney, mice were administered OGC-3 and PTX-OGC-3 i.v. at the dose that was half of the LD<sub>50</sub>. The histopathological changes in each organ were observed under light microscopy on day 8 after treatment with OGC-3 or PTX-OGC-3 (Fig. 8). No histopathological changes were observed in the OGC-3 or PTX-OGC-3-treated groups compared to the control group, which indicated that both OGC micelles and PTX-loaded OGC micelles had no significant toxicity for the main organs.

### 3.6. Cytotoxicity

The cytotoxicity of PTX-loaded and PTX-free OGC micelles against human hepatoma HepG2 cells was evaluated using the MTT method. For comparison, the cytotoxicity of blank micelles, Taxol and its vehicle (Cremophor EL/ethanol = 50/50 (v/v), abbreviated as Taxol vehicle), and pure PTX solution was also evaluated. As shown in Fig. 9a, blank micelles did not show any toxicity, even at the highest concentration tested, while strong cytotoxicity was observed when the cells were incubated in the presence of a concentrated Taxol vehicle. Therefore, it can be expected that OGC micelles are far less toxic than Cremophor EL vehicle.

As shown in Fig. 9b, the PTX-loaded micelles showed comparable cytotoxicity as PTX formulated with Cremophor EL/ethanol, which indicated that PTX remained biologically active after being incorporated into OGC micelles. Taxol showed strong cytotoxicity at 100 and 10  $\mu$ g/mL, which may be attributed partially to the use

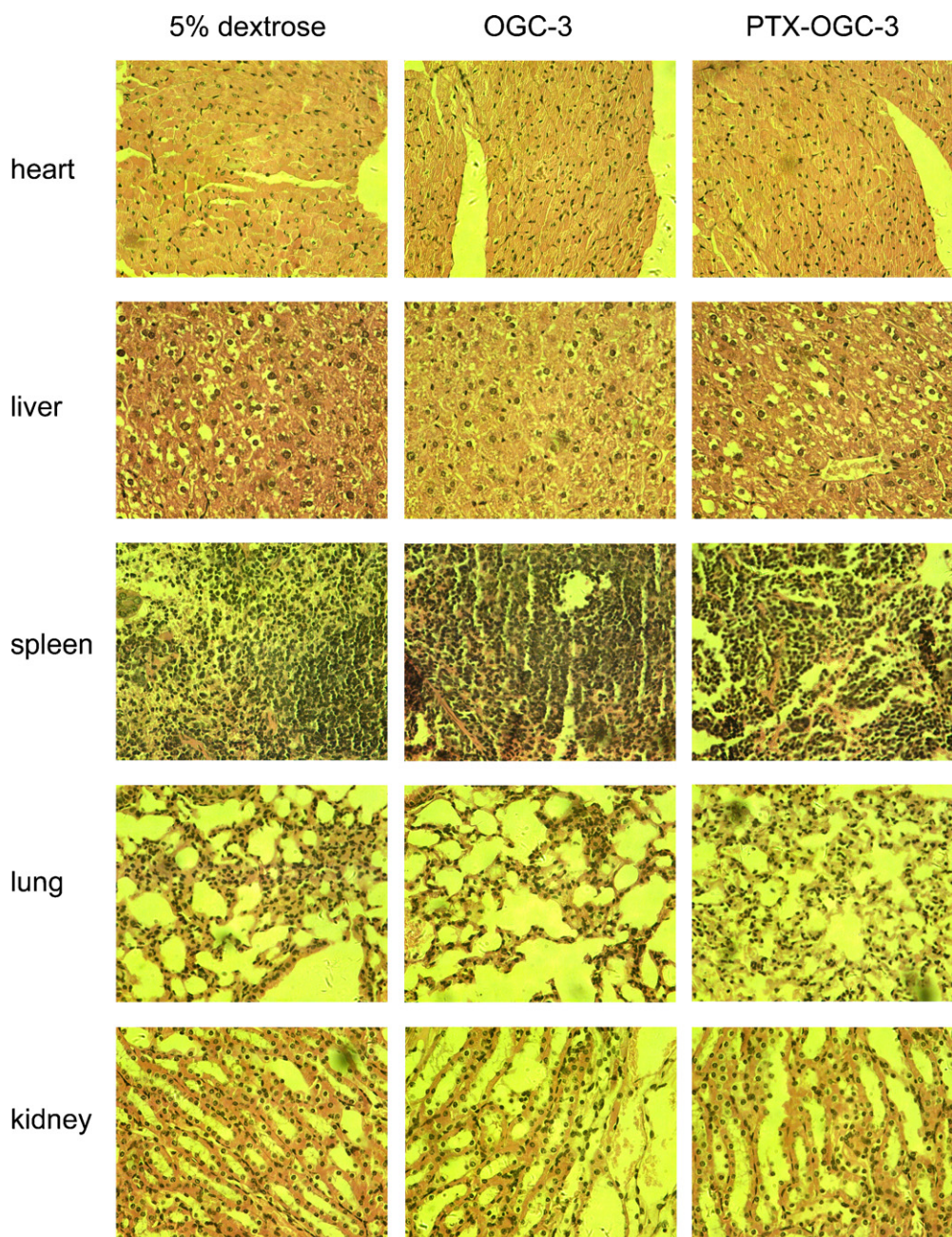
**Table 3**

Determination of MTD at day 7 after i.v. injection of a single dose.

Formulations	Taxol				PTX-OGC-3 (32.8 wt.%)			
	20	25	30	40	80	90	100	110
Deaths	0/10	0/10	0/10	1/10	0/10	0/10	0/10	1/10
Observation postinjection	Apathy, catatonia, prostration	Apathy, catatonia, prostration	Apathy, catatonia, prostration	Apathy, catatonia, prostration	No apathy	No apathy	No apathy	No apathy
Body weight loss (%)	<5	<10	>10	>10	<5	<5	<5	<5

of Cremophor EL vehicle. In contrast, the cytotoxicity of PTX-loaded micelles was more likely induced by PTX itself. Cytotoxicity of free PTX at a concentration of 10 and 100  $\mu\text{g/mL}$  was not tested because of its low solubility in cell culture medium. It should be mentioned that PTX-loaded micelles exhibited higher cytotoxicity than the pure PTX solutions did at concentrations of 0.1 and 1  $\mu\text{g/mL}$ , and

this might have been attributed to the enhanced permeability of the cell membrane induced by OGC amphiphiles, which resulted in more drug being taken up by the cells. The  $\text{IC}_{50}$  of PTX-OGC-1, PTX-OGC-2 and PTX-OGC-3 was 0.21 ( $\pm 0.07$ ), 0.19 ( $\pm 0.09$ ) and 0.28 ( $\pm 0.14$ )  $\mu\text{g/mL}$  respectively, which was lower than that of Taxol whose  $\text{IC}_{50}$  was 0.79 ( $\pm 0.36$ )  $\mu\text{g/mL}$ . But no significant difference

**Fig. 8.** Microphotographs of the organs of the mice treated with 5% dextrose, OGC-3 or PTX-OGC-3 ( $\times 500$ ).



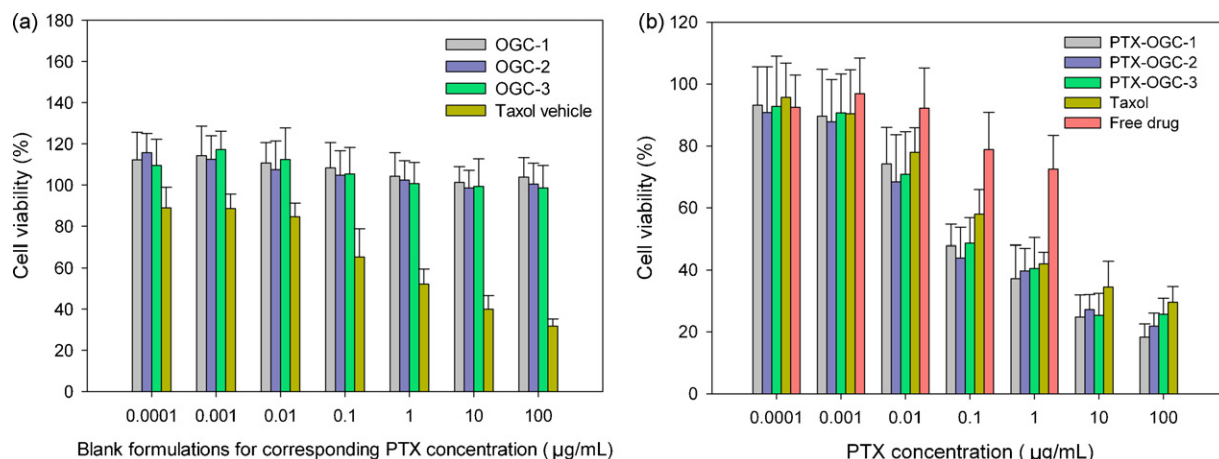


**Fig. 9.** Cell viability after 72 h incubation with (a) blank formulations for corresponding PTX concentration varies from 0.0001 to 100 µg/mL; (b) PTX-loaded OGC micelles, Taxol and free PTX.

was observed among these formulations ( $P > 0.05$ ). Based on these cytotoxicity results, it can be concluded that PTX-loaded polymeric micelles were equipotent to the commercial PTX formulation and that OGC was less cytotoxic than Taxol vehicle in the absence of drug.

#### 4. Conclusions

In this study, novel nanomicelles based on glycol chitosan bearing various amounts of alkyl chains were synthesized and characterized. OGC exhibited a low CMC, above which the amphiphilic derivatives self-assembled in an aqueous environment to form micelles. The biocompatibility and nontoxicity of OGC as excipient for the formulations aiming at i.v. administration were confirmed in this study. Furthermore, PTX, a water-insoluble antitumor drug, was successfully loaded into OGC micelles by using a simple dialysis method. The drug-loading capacity of OGC was significantly affected by the DS of alkyl chains. The superior features of the PTX-loaded OGC micellar system over other polymeric micelles were its high drug-loading capacity (32.8 wt.%), high drug-loading efficiency (91.9%), and enhanced long-term stability in aqueous solution (5 days). Furthermore, a series of safety studies revealed that PTX-loaded OGC micelles had advantages over the commercially available injectable preparation of PTX (Taxol) in terms of low toxicity levels and increased tolerated dose. In addition, the MTT assay showed that the *in vitro* cytotoxic effect of the PTX-loaded micelles was comparable to that of the commercial formulation, but the blank micelles were far less toxic than the Cremophor EL vehicle. The results of this research demonstrate the potential of OGC as an alternative and promising carrier for micelles of PTX and other similar hydrophobic anticancer agents.

#### Acknowledgements

The authors thank the financial support provided by the Natural Science Foundation of Jiangsu Province (No. BK2007173), Specialized Research Fund for the Doctoral Program of Advanced Education of China (No. 200803161017), and Key New Drug Innovation Project from the Ministry of Science and Technology of the People's Republic of China (No. 2009ZX09310-004). The authors wish to thank Dr. David L. Armbruster (The University of Tennessee Health Sciences Center, USA) for his kind editorial help in revising the writing of this article.

#### References

- Alexis, F., Pridgen, E., Molnar, L.K., Farokhzad, O.C., 2008. Factors affecting the clearance and biodistribution of polymeric nanoparticles. *Mol. Pharm.* 5, 505–515.
- Bliss, C.L., 1935. The calculation of the dosage mortality curve. *Ann. Appl. Biol.* 22, 134–167.
- Bouquet, W., Ceelen, W., Fritzinger, B., Pattyn, P., Peeters, M., Remon, J.P., Vervaeke, C., 2007. Paclitaxel/beta-cyclodextrin complexes for hyperthermic peritoneal perfusion—formulation and stability. *Eur. J. Pharm. Biopharm.* 66, 391–397.
- Branco, M.C., Schneider, J.P., 2009. Self-assembling materials for therapeutic delivery. *Acta Biomater.* 5, 817–831.
- Burt, H.M., Zhang, X., Toleikis, P., Embree, L., WL, H., 1999. Development of copolymers of poly(D,L-lactide) and methoxypolyethylene glycol as micellar carriers of paclitaxel. *Colloids Surf. B: Biointerfaces* 16, 161–171.
- Carstens, M.G., de Jong, P.H., van Nostrum, C.F., Kemmink, J., Verrijck, R., de Leede, L.G., Crommelin, D.J., Hennink, W.E., 2008. The effect of core composition in biodegradable oligomeric micelles as taxane formulations. *Eur. J. Pharm. Biopharm.* 68, 596–606.
- Cavallaro, G., Licciardi, M., Giammona, G., Caliceti, P., Semenzato, A., Salmaso, S., 2003. Poly(hydroxyethylaspartamide) derivatives as colloidal drug carrier systems. *J. Control. Rel.* 89, 285–295.
- Chen, S.C., Wu, Y.C., Mi, F.L., Lin, Y.H., Yu, L.C., Sung, H.W., 2004. A novel pH-sensitive hydrogel composed of N,O-carboxymethyl chitosan and alginate cross-linked by genipin for protein drug delivery. *J. Control. Rel.* 96, 285–300.
- Chen, X.G., Lee, C.M., Park, H.J., 2003. O/W emulsification for the self-aggregation and nanoparticle formation of linoleic acid-modified chitosan in the aqueous system. *J. Agric. Food Chem.* 51, 3135–3139.
- Cheon Lee, S., Kim, C., Chan Kwon, I., Chung, H., Young Jeong, S., 2003. Polymeric micelles of poly(2-ethyl-2-oxazoline)-block-poly(epsilon-caprolactone) copolymer as a carrier for paclitaxel. *J. Control. Rel.* 89, 437–446.
- Cheong, S.J., Lee, C.M., Kim, S.L., Jeong, H.J., Kim, E.M., Park, E.H., Kim, D.W., Lim, S.T., Sohn, M.H., 2009. Superparamagnetic iron oxide nanoparticles-loaded chitosan-linoleic acid nanoparticles as an effective hepatocyte-targeted gene delivery system. *Int. J. Pharm.* 372, 169–176.
- Danhier, F., Magotteaux, N., Ucakar, B., Lecouturier, N., Brewster, M., Preat, V., 2009. Novel self-assembling PEG-p(CL-co-TMC) polymeric micelles as safe and effective delivery system for paclitaxel. *Eur. J. Pharm. Biopharm.* 73, 230–238.
- Diaz, C., Vargas, E., Gattens-Boniche, O., 2006. Cytotoxic effect induced by retinoic acid loaded into galactosyl-sphingosine containing liposomes on human hepatoma cell lines. *Int. J. Pharm.* 325, 108–115.
- Du, Y.Z., Wang, L., Yuan, H., Wei, X.H., Hu, F.Q., 2009. Preparation and characteristics of linoleic acid-grafted chitosan oligosaccharide micelles as a carrier for doxorubicin. *Colloids Surf. B: Biointerfaces* 69, 257–263.
- Fahr, A., Liu, X., 2007. Drug delivery strategies for poorly water-soluble drugs. *Expert Opin. Drug Deliv.* 4, 403–416.
- Feng, S., Huang, G., 2001. Effects of emulsifiers on the controlled release of paclitaxel (Taxol) from nanospheres of biodegradable polymers. *J. Control. Rel.* 71, 53–69.
- Fransson, M., Green, H., 2008. Comparison of two types of population pharmacokinetic model structures of paclitaxel. *Eur. J. Pharm. Sci.* 33, 128–137.
- Freireich, E.J., Gehan, E.A., Rall, D.P., Schmidt, L.H., Skipper, H.E., 1966. Quantitative comparison of toxicity of anticancer agents in mouse, rat, hamster, dog, monkey, and man. *Cancer Chemother. Rep.* 50, 219–244.
- Gao, J., Ming, J., He, B., Fan, Y., Gu, Z., Zhang, X., 2008. Preparation and characterization of novel polymeric micelles for 9-nitro-20(S)-camptothecin delivery. *Eur. J. Pharm. Sci.* 34, 85–93.
- Gelderblom, H., Verweij, J., Nooter, K., Sparreboom, A., 2001. Cremophor EL: the drawbacks and advantages of vehicle selection for drug formulation. *Eur. J. Cancer.* 37, 1590–1598.
- Han, J., Washington, C., Davis, S.S., 2007. Design and evaluation of an emulsion vehicle for paclitaxel. II. Suppression of the crystallization of

- paclitaxel by freeze-drying technique. *Drug Dev. Ind. Pharm.* 33, 1151–1157.
- Hu, F.Q., Li, Y.H., Yuan, H., Zeng, S., 2006a. Novel self-aggregates of chitosan oligosaccharide grafted stearic acid: preparation, characterization and protein association. *Pharmazie* 61, 194–198.
- Hu, F.Q., Meng, P., Dai, Y.Q., Du, Y.Z., You, J., Wei, X.H., Yuan, H., 2008a. PEGylated chitosan-based polymer micelle as an intracellular delivery carrier for anti-tumor targeting therapy. *Eur. J. Pharm. Biopharm.* 70, 749–757.
- Hu, F.Q., Ren, G.F., Yuan, H., Du, Y.Z., Zeng, S., 2006b. Shell cross-linked stearic acid grafted chitosan oligosaccharide self-aggregated micelles for controlled release of paclitaxel. *Colloids Surf. B: Biointerfaces* 50, 97–103.
- Hu, F.Q., Wu, X.L., Du, Y.Z., You, J., Yuan, H., 2008b. Cellular uptake and cytotoxicity of shell crosslinked stearic acid-grafted chitosan oligosaccharide micelles encapsulating doxorubicin. *Eur. J. Pharm. Biopharm.* 69, 117–125.
- Hu, F.Q., Zhao, M.D., Yuan, H., You, J., Du, Y.Z., Zeng, S., 2006c. A novel chitosan oligosaccharide-stearic acid micelles for gene delivery: properties and in vitro transfection studies. *Int. J. Pharm.* 315, 158–166.
- Huang, M.F., Shen, W.Q., Fang, Y., 2005. Synthesis of a novel chitosan derivative having poly (ethylene oxide) side chains in aqueous reaction media. *React. Funct. Polym.* 65, 301–308.
- Huh, K.M., Lee, S.C., Cho, Y.W., Lee, J., Jeong, J.H., Park, K., 2005. Hydrotropic polymer micelle system for delivery of paclitaxel. *J. Control. Rel.* 101, 59–68.
- Kadam, Y., Yerramilli, U., Bahadur, A., 2009. Solubilization of poorly water-soluble drug carbamazepine in pluronic micelles: effect of molecular characteristics, temperature and added salt on the solubilizing capacity. *Colloids Surf. B: Biointerfaces* 72, 141–147.
- Kakinoki, A., Kaneo, Y., Tanaka, T., Hosokawa, Y., 2008. Synthesis and evaluation of water-soluble poly(vinyl alcohol)-paclitaxel conjugate as a macromolecular prodrug. *Biol. Pharm. Bull.* 31, 963–969.
- Kawano, K., Watanabe, M., Yamamoto, T., Yokoyama, M., Opanasopit, P., Okano, T., Maitani, Y., 2006. Enhanced antitumor effect of camptothecin loaded in long-circulating polymeric micelles. *J. Control. Rel.* 112, 329–332.
- Kim, J.H., Kim, Y.S., Kim, S., Park, J.H., Kim, K., Choi, K., Chung, H., Jeong, S.Y., Park, R.W., Kim, I.S., Kwon, I.C., 2006. Hydrophobically modified glycol chitosan nanoparticles as carriers for paclitaxel. *J. Control. Rel.* 111, 228–234.
- Kim, K., Kwon, S., Hyung Park, J., Chung, H., Young Jeong, S., 2003. Physicochemical characteristics of self-assembled nanoparticles based on glycol chitosan bearing 5 $\beta$ -cholanolic acid. *Langmuir*, 10188–10193.
- Kim, K., Kwon, S., Park, J.H., Chung, H., Jeong, S.Y., Kwon, I.C., Kim, I.S., 2005a. Physicochemical characterizations of self-assembled nanoparticles of glycol chitosan-deoxycholic acid conjugates. *Biomacromolecules* 6, 1154–1158.
- Kim, S.C., Yoon, H.J., Lee, J.W., Yu, J., Park, E.S., Chi, S.C., 2005b. Investigation of the release behavior of DEHP from infusion sets by paclitaxel-loaded polymeric micelles. *Int. J. Pharm.* 293, 303–310.
- Kumar, G., Bristow, J.F., Smith, P.J., Payne, G.F., 2000. Enzymatic gelation of the natural polymer chitosan. *Polymer* 41, 2157–2168.
- Le Garrec, D., Gori, S., Luo, L., Lessard, D., Smith, D.C., Yessine, M.A., Ranger, M., Leroux, J.C., 2004. Poly(N-vinylpyrrolidone)-block-poly(D,L-lactide) as a new polymeric solubilizer for hydrophobic anticancer drugs: in vitro and in vivo evaluation. *J. Control. Rel.* 99, 83–101.
- Lee, K.Y., Jo, W.H., Kwon, I.C., Kim, Y.H., Jeong, S.Y., 1998. Structural determination and interior polarity of self-aggregates prepared from deoxycholic acid-modified chitosan in water. *Macromolecules* 31, 378–383.
- Lee, K.Y., Kwon, I.C., Jo, W.H., Jeong, S.Y., 2005. Complex formation between plasmid DNA and self-aggregates of deoxycholic acid-modified chitosan. *Polymer* 46, 8107–8112.
- Lee, S.J., Park, K., Oh, Y.K., Kwon, S.H., Her, S., Kim, I.S., Choi, K., Lee, S.J., Kim, H., Lee, S.G., Kim, K., Kwon, I.C., 2009. Tumor specificity and therapeutic efficacy of photosensitizer-encapsulated glycol chitosan-based nanoparticles in tumor-bearing mice. *Biomaterials* 30, 2929–2939.
- Li, S., Byrne, B., Welsh, J., Palmer, A.F., 2007. Self-assembled poly(butadiene)-b-poly(ethylene oxide) polymersomes as paclitaxel carriers. *Biotechnol. Prog.* 23, 278–285.
- Licciardi, M., Giammona, G., Du, J., Armes, S.P., Tang, Y., Lewis, A.L., 2006. New folate-functionalized biocompatible block copolymer micelles as potential anti-cancer drug delivery systems. *Polymer* 47, 2946–2955.
- Liggins, R.T., Burt, H.M., 2002. Polyether-polyester diblock copolymers for the preparation of paclitaxel loaded polymeric micelle formulations. *Adv. Drug Deliv. Rev.* 54, 191–202.
- Liu, C.G., Desai, K.G., Chen, X.G., Park, H.J., 2005. Linolenic acid-modified chitosan for formation of self-assembled nanoparticles. *J. Agric. Food Chem.* 53, 437–441.
- Liu, T.Y., Chen, S.Y., Lin, Y.L., Liu, D.M., 2006. Synthesis and characterization of amphiphatic carboxymethyl-hexanoyl chitosan hydrogel: water-retention ability and drug encapsulation. *Langmuir* 22, 9740–9745.
- Liu, W., Sun, S.J., Zhang, X., Yao, K.D., 2003. Self-aggregation behavior of alkylated chitosan and its effect on the release of a hydrophobic drug. *J. Biomater. Sci. Polym. Ed.* 14, 851–859.
- Mahmud, A., Xiong, X.B., Aliabadi, H.M., Lavasanifar, A., 2007. Polymeric micelles for drug targeting. *J. Drug Target* 15, 553–584.
- Marcel Musteata, F., Pawliszyn, J., 2006. Determination of free concentration of Paclitaxel in liposome formulation. *J. Pharm. Pharm. Sci.* 9, 231–237.
- Mi, F.L., Tan, Y.C., Liang, H.F., Sung, H.W., 2002. In vivo biocompatibility and degradability of a novel injectable-chitosan-based implant. *Biomaterials* 23, 181–191.
- Min, K.H., Park, K., Kim, Y.S., Bae, S.M., Lee, S., Jo, H.G., Park, R.W., Kim, I.S., Jeong, S.Y., Kim, K., Kwon, I.C., 2008. Hydrophobically modified glycol chitosan nanoparticles-encapsulated camptothecin enhance the drug stability and tumor targeting in cancer therapy. *J. Control. Rel.* 127, 208–218.
- Miwa, A., Ishibe, A., Nakano, M., Yamahira, T., Itai, S., Jinno, S., Kawahara, H., 1998. Development of novel chitosan derivatives as micellar carriers of Taxol. *Pharm. Res.* 15, 1844–1850.
- Nam, H.Y., Kwon, S.M., Chung, H., Lee, S.Y., Kwon, S.H., Jeon, H., Kim, Y., Park, J.H., Kim, J., Her, S., Oh, Y.K., Kwon, I.C., Kim, K., Jeong, S.Y., 2009. Cellular uptake mechanism and intracellular fate of hydrophobically modified glycol chitosan nanoparticles. *J. Control. Rel.* 135, 259–267.
- Pourroy, B., Botta, C., Solas, C., Lacarelle, B., Braguer, D., 2005. Seventy-two-hour stability of Taxol in 5% dextrose or 0.9% sodium chloride in Viallo, Freeflex, Ecoflac and Macoflex N non-PVC bags. *J. Clin. Pharm. Ther.* 30, 455–458.
- Qiu, L.Y., Wu, X.L., Jin, Y., 2009. Doxorubicin-loaded polymeric micelles based on amphiphilic polyphosphazenes with poly(N-isopropylacrylamide-co-N,N-dimethylacrylamide) and ethyl glycinate as side groups: synthesis, preparation and in vitro evaluation. *Pharm. Res.* 26, 946–957.
- Saravanakumar, G., Min, K.H., Min, D.S., Kim, A.Y., Lee, C.M., Cho, Y.W., Lee, S.C., Kim, K., Jeong, S.Y., Park, K., Park, J.H., Kwon, I.C., 2009. Hydrotropic oligomer-conjugated glycol chitosan as a carrier of paclitaxel: synthesis, characterization, and in vivo biodistribution. *J. Control. Rel.* 140, 210–217.
- Senso, A., Franco, P., Oliveros, L., Minguillon, C.A., 2000. Characterization of doubly substituted polysaccharide derivatives. *Carbohydr. Res.* 329, 367–376.
- Seow, W.Y., Xue, J.M., Yang, Y.Y., 2007. Targeted and intracellular delivery of paclitaxel using multi-functional polymeric micelles. *Biomaterials* 28, 1730–1740.
- Stanford, B.L., Hardwicke, F., 2003. A review of clinical experience with paclitaxel extravasations. *Support Care Cancer* 11, 270–277.
- Wang, Y., Li, Y., Wang, Q., Wu, J., Fang, X., 2008. Pharmacokinetics and biodistribution of paclitaxel-loaded pluronic P105/L101 mixed polymeric micelles. *Yakugaku Zasshi* 128, 941–950.
- Wilhelm, M., Zhao, C., Wang, Y., Xu, R., Winnik, M.A., Mura, J., 1991. Poly(styrene-ethylene oxide) block copolymer micelle formation in water: a fluorescence probe study. *Macromolecules*, 1033–1044.
- Xu, X.Y., Li, L., Zhou, J.P., Lu, S.Y., Yang, J., Yin, X.J., Ren, J.S., 2007. Preparation and characterization of N-succinyl-N'-octyl chitosan micelles as doxorubicin carriers for effective anti-tumor activity. *Colloids Surf. B: Biointerfaces* 55, 222–228.
- Ye, Y.Q., Chen, F.Y., Wu, Q.A., Hu, F.Q., Du, Y.Z., Yuan, H., Yu, H.Y., 2009. Enhanced cytotoxicity of core modified chitosan based polymeric micelles for doxorubicin delivery. *J. Pharm. Sci.* 98, 704–712.
- Zhang, C., Qineng, P., Zhang, H., 2004. Self-assembly and characterization of paclitaxel-loaded N-octyl-O-sulfate chitosan micellar system. *Colloids Surf. B: Biointerfaces* 39, 69–75.
- Zhang, Y., Huo, M.R., Zhou, J.P., Yu, D., Wu, Y.P., 2009. Potential of amphiphilically modified low molecular weight chitosan as a novel carrier for hydrophobic anticancer drug: synthesis, characterization, micellization and cytotoxicity evaluation. *Carbohydr. Polym.* 77, 231–238.
- Zhao, Z., He, M., Yin, L., Bao, J., Shi, L., Wang, B., Tang, C., Yin, C., 2009. Biodegradable nanoparticles based on linoleic acid and poly(beta-malic acid) double grafted chitosan derivatives as carriers of anticancer drugs. *Biomacromolecules* 10, 565–572.